Available online at www.sciencedirect.com
ScienceDirect
Metabolism Clinical and Experimental 59 (2010) 1000 – 1011
Metabolism
Clinical and Experimental
www.metabolismjournal.com

Methionine restriction effects on mitochondrial biogenesis and aerobic capacity in white adipose tissue, liver, and skeletal muscle of F344 rats

Carmen E. Perrone*, Dwight A.L. Mattocks, Maureen Jarvis-Morar, Jason D. Plummer, Norman Orentreich

Orentreich Foundation for the Advancement of Science, Inc., Cold Spring-on-Hudson, NY 10516, USA

Received 2 July 2009; accepted 26 October 2009

Abstract

Methionine restriction increases life span in rats and mice and reduces age-related accretion of adipose tissue in Fischer 344 rats. Recent reports have shown that adipose tissue mitochondrial content and function are associated with adiposity; therefore, the expression of genes involved in mitochondrial biogenesis and oxidative capacity was examined in white adipose tissue, liver, and skeletal muscle from Fischer 344 rats fed control (0.86% methionine) or methionine-restricted (0.17% methionine) diets for 3 months. Methionine restriction induced transcriptional changes of peroxisome proliferator-activated receptors, peroxisome proliferator-activated receptor coactivators 1α and 1β, and some of their known target genes in all of these tissues. In addition, tissue-specific responses were elicited at the protein level. In inguinal adipose tissue, methionine restriction increased protein levels of peroxisome proliferator-activated receptor and peroxisome proliferator-activated receptor coactivator target genes. It also induced mitochondrial DNA copy number, suggesting mitochondrial biogenesis and corresponding with the up-regulation of citrate synthase activity. In contrast, methionine restriction induced changes in mitochondrial glycerol-3-phosphate dehydrogenase activity and stearoyl–coenzyme A desaturase 1 protein levels only in liver and uncoupling protein 3 and cytochrome *c* oxidase subunit IV protein levels only in skeletal muscle. No increase in mitochondrial DNA copy number was observed in liver and skeletal muscle despite an increase in mitochondrial citrate synthase activity. The results indicate that adiposity resistance in methionine-restricted rats is associated with mitochondrial biogenesis in inguinal adipose tissue and increased mitochondrial aerobic capacity in liver and skeletal muscle.
Published by Elsevier Inc.

1. Introduction

Methionine restriction (MR) is a dietary regimen that extends life span [1] and delays the onset of age-related diseases [2]. Methionine restriction also limits age-related increases of adipose tissue (AT) mass in male Fischer 344 (F344) rats [3]. This is a specific response to reduced methionine intake and is not due to caloric restriction because, per gram of body weight, MR rats consume more food than age-matched control-fed (CF) rats [3,4], and growth and key adiposity markers are not changed in rats pair-fed the quantity of food consumed by MR rats [3]. Furthermore, increased energy expenditure [3] and changes in AT lipogenic/lipolytic balance leading to a lipid futile cycle [5] are also observed in MR rats, suggesting that adiposity resistance (AR) may be associated with a negative energy balance.

Adiposity resistance in rodents positively correlates with mitochondrial biogenesis and oxidative phosphorylation [6,7]. Mitochondria are central players in energy metabolism, fatty acid oxidation, and body fat distribution [8,9]; and there is increasing evidence that mitochondrial dysfunction is involved in the development and perpetuation of obesity [10-12]. Although most studies have emphasized the relationship between obesity and mitochondrial dysfunction in tissues with high oxidative capacities such as skeletal muscle, there are also reports showing decreased mitochon-

* Corresponding author. Cell Biology Laboratory, Biomedical Research Station, Orentreich Foundation for the Advancement of Science, Inc., Cold Spring-on-Hudson, NY 10516, USA. Tel.: +1 845 265 4200x235; fax: +1 845 265 4210.

E-mail addresses: perrone@orentreich.org, perronecepr@yahoo.com (C.E. Perrone).

0026-0495/$ – see front matter. Published by Elsevier Inc.
doi:10.1016/j.metabol.2009.10.023

drial number and activity in AT of obese humans and animal models [13-15].

Reduced mitochondrial number and function in AT from obese patients and rodents are associated with the decreased expression of the peroxisome proliferator-activated receptor γ coactivator 1α (*Ppargc1a*; PGC1α) [13,14,16,17]. Peroxisome proliferator-activated receptor γ coactivator 1α overexpression in white AT (WAT) stimulates mitochondrial biogenesis and up-regulates genes that increase energy metabolism [18,19]. Its homologue, PGC1*β*, is constitutively expressed and complements PGC1α's effects on mitochondrial biogenesis [20,21]. *Ppargc1b* overexpression in mice also induces a lean phenotype despite the mice being hyperphagic [22] and reduces serum leptin, correlating with a decrease in AT mass and an improvement in insulin and glucose sensitivity [22].

Peroxisome proliferator-activated receptor γ coactivator 1α exerts its pleiotropic effects on mitochondrial biogenesis and oxidative capacity through the coactivation of nuclear receptors such as the nuclear respiratory factors (NRFs), estrogen-related receptors (ERRs), and peroxisome proliferator-activated receptors (PPARs) among others [23-25]. Nuclear respiratory factors 1 and 2 control the expression of mitochondrial transcription factor A (*Tfam*), which is essential for the replication, maintenance, and transcription of mitochondrial DNA (mtDNA) [26,27] as well as the expression of nuclear genes encoding mitochondrial respiratory chain subunits [28]. Estrogen-related receptor α has been implicated in fatty acid *β*-oxidation because it is a direct regulator of the medium-chain acyl–coenzyme A (CoA) dehydrogenase (MCAD) gene (*Acadm*) [29].

There are 3 differentially expressed PPAR isotypes (PPARα, *β*/*δ*, and γ), all of which are PGC1α targets [30] and are expressed in AT where they determine the number of adipocytes and their capacity to store triglycerides [25,31,32]. Peroxisome proliferator-activated receptor *β*/*δ* controls preadipocyte proliferation and *Pparg* gene expression [25], and activation of PPARγ induces WAT remodeling (characterized by an increased number of smaller insulin-sensitive adipocytes) and up-regulates lipogenesis and triglyceride storage [31,33]. Peroxisome proliferator-activated receptor γ activation also induces uncoupling protein 1 (*Ucp1*), carnitine palmitoyltransferase 1 (*Cpt1*), and *Ppara* gene expression, as well as adrenergic sensitization in brown AT [34-36]. Peroxisome proliferator-activated receptor α activation also increases the expression of genes involved in mitochondrial fatty acid oxidation including *Cpt1* [37].

Studies were conducted to examine whether AR in MR rats is associated with the transcriptional regulation of genes linked to mitochondrial biogenesis and oxidative capacity. The expression of *Ppargc1*s, *Ppars*, and some of their known target genes was measured in ATs, liver, and skeletal muscle by quantitative reverse transcriptase polymerase chain reaction (qPCR); and levels of proteins corresponding to genes expression changes by MR were evaluated by Western blotting. Mitochondrial biogenesis was assessed as a function of mtDNA copy number via real-time PCR, and mitochondrial aerobic capacity was determined by measuring the activity of the mitochondrial matrix enzyme citrate synthase.

2. Materials and methods

All studies were reviewed and approved by the Institutional Animal Care and Use Committee of the Orentreich Foundation for the Advancement of Science and performed in accordance with the National Institutes of Health's guidelines for the use of animals in research laboratories.

2.1. Materials

Chemically defined diets based on the AIN-76 diet with protein replaced by amino acid mixtures containing either 0.86% or 0.17% methionine [1,38] were purchased from Dyets (Bethlehem, PA). RNeasy Kits and DNeasy Blood and Tissue Kits were obtained from Qiagen (Valencia, CA). High-Capacity complementary DNA (cDNA) Reverse Transcription Kits, TaqMan Gene Expression Master Mix, RT-PCR–grade water, and TaqMan primer-probe sets (Table S1) were purchased from Applied Biosystems (Foster City, CA). Halt Protease and Phosphatase Inhibitors, West Pico and West Femto Chemiluminescence Kits, BCA (standard and reducing agent compatible) Protein Assay Kits, and the ERRα antibody (Ab) were obtained from Pierce (Rockford, IL). Acrylamide, blotting paper, polyvinyldifluoride membranes, 10% Tween 20, and horseradish peroxidase–conjugated anti-rabbit and anti-mouse immunoglobulin Gs were from BioRad (Hercules, CA). Antibodies raised against MCAD, myoglobin, pyruvate dehydrogenase kinase 4 (PDK4), PPAR*β*/*δ*, slow-twitch troponin, tubulin, UCP1, and UCP3 were from Abcam (Cambridge, MA). The PPARγ Ab was from GeneTex (San Antonio, TX); and fatty acid binding protein 4 (FABP4), PPARα, and PGC1 Abs were from Cayman Chemical (Ann Arbor, MI). BLOTTO and cytochrome *c* oxidase subunit IV (COX4) and stearoyl-CoA desaturase 1 (SCD1) Abs were from Santa Cruz Biotechnology (Santa Cruz, CA). Adrenergic receptor *β*3 (Adr*β*3) and horseradish peroxidase–conjugated anti-chicken immunoglobulin G Abs were from Chemicon International (Temecula, CA). The *β*-actin Ab and all other chemicals were purchased from Sigma-Aldrich (St Louis, MO) unless otherwise specified.

2.2. Animal husbandry, tissue collection, and serum parameters

Four-week-old male F344 rats obtained from Taconic Farms (Germantown, NY) were maintained 1 rat per cage on a 12-hour light-dark cycle and fed Laboratory Rodent Diet (5001; PMI Nutrition International, Brentwood, MO) for 2 weeks. At 6 weeks of age, the rats were randomly assigned to control or MR diets (n = 7 per treatment group); and food and

water were provided ad libitum. After 3 months on these dietary regimens, the rats were anesthetized; and blood was collected from the subclavian vein. The rats were then euthanized; and ATs (inguinal, epididymal, and retroperitoneal fat), liver, and skeletal (quadriceps) muscle were immediately harvested, weighed, frozen in liquid nitrogen, and stored at −80°C. The rats were not fasted before tissue collection. Serum metabolites and hormones were measured as previously described [3,5].

2.3. Gene expression

Total RNA was isolated from 7 independent samples per tissue type using Qiagen RNeasy Kits, the RNA concentrations were determined spectrophotometrically, and their integrity was assessed by agarose gel electrophoresis. Messenger RNA (mRNA) was transcribed into cDNA with the High-Capacity cDNA Reverse Transcription Kit in a Perkin-Elmer (Wellesley, MA) GeneAmp PCR System 9600 using the following parameters: 1 cycle at 25°C for 10 minutes, followed by 1 cycle at 37°C for 120 minutes and 1 cycle at 85°C for 5 seconds. The cDNA was then used in multiplexed PCR that was performed in a StepOne Real-Time PCR System using commercially available primer-probe sets (Table S1, Applied Biosystems). The PCR parameters were as follows: 1 cycle at 50°C for 2 minutes and 95°C for 10 minutes, followed by 40 cycles at 95°C for 15 seconds and 60°C for 1 minute. Gene expression was assessed via the comparative C_T ($\Delta\Delta C_T$) method with β-actin as the reference gene. β-Actin C_T values were approximately the same in tissues from CF and MR rats, and efficiencies for β-actin and the genes of interest in the multiplexed reactions were greater than 90%.

2.4. Western blots

For cytosolic and mitochondrial protein Western blots, ATs were homogenized with a Polytron-type homogenizer in a sucrose-EDTA-Tris-magnesium buffer (SET-Mg buffer; 10% sucrose, 1 mmol/L EDTA, 6 mmol/L $MgCl_2$, 50 mmol/L Tris-HCl buffer, pH 7.2) containing protease and phosphatase inhibitors. The homogenates were sonicated and centrifuged at 100*g* for 5 minutes at 4°C, and infranatants were collected and stored at −20°C. For nuclear protein determinations, ATs were processed via a modification of the protocol reported by Ström et al [39] for PPARγ Western blots. Briefly, the tissues were homogenized in sucrose-EDTA buffer (250 mmol/L sucrose, 1 mmol/L EDTA, pH 7.0) containing 1 mmol/L dithiothreitol and protease inhibitors; and the homogenates were centrifuged at 16 000*g* for 25 minutes at 4°C. The resulting pellets were resuspended in homogenization buffer containing 5% sodium dodecyl sulfate (SDS) and incubated for 30 minutes at 50°C. After the 50°C incubation, the samples were sonicated and centrifuged at 200*g* for 5 minutes. The supernatants were collected and stored at −20°C. Liver and skeletal muscle Western blots were conducted using whole homogenates prepared in SET-Mg buffer as described above for AT.

Fifty micrograms of protein was electrophoresed in 4% to 20% SDS–polyacrylamide gel electrophoresis gradient gels for cytosolic and mitochondrial protein Western blots; for nuclear protein Western blots, 75 to 100 μg of protein was resolved in 7.5% gels. For each tissue, 7 samples were analyzed per treatment group. The proteins were transferred to polyvinyldifluoride membranes that were blocked with 5% BLOTTO in TBS–0.1% Tween, and then incubated with the appropriate primary Ab. The membranes were incubated in appropriate secondary Abs and developed using the West Pico or West Femto enhanced chemiluminescence substrates. The COX4, FABP4, and ERRα proteins were detected by the West Pico substrate using secondary Ab dilutions of 1:5000 to 1:20,000. All other proteins were detected with the West Femto kit using secondary Ab dilutions ranging from 1:200 000 to 1:500 000. Densitometry measurements of protein bands were analyzed with UN-Scan-It Gel version 6.1 (Silk Scientific, Orem, UT) and normalized with β-actin or α-tubulin as loading controls for AT and liver or skeletal muscle, respectively.

2.5. Enzyme assays

The CPT1 enzyme activity was measured using modifications of the methods of McGarry et al [40] and Zierz and Engel [41] as reported by Kim et al [42]. Tissues were homogenized in SET buffer, and the homogenates were centrifuged at 100*g* for 5 minutes at 4°C. The AT infranatants and liver and skeletal muscle supernatants were collected and stored at −80°C until assayed. Protein content was determined with the BCA Protein Assay Kit, and various concentrations of proteins were preincubated at 30°C for 10 minutes in microcentrifuge tubes. Reaction buffer (117 mmol/L Tris-HCl, pH 7.4, 0.28 mmol/L reduced glutathione, 4.4 mmol/L adenosine triphosphate, 4.4 mmol/L $MgCl_2$, 16.7 mmol/L KCl, 2.2 mmol/L KCN, 40 mg/L rotenone, 0.1% defatted bovine serum albumin, 50 μmol/L palmitoyl-CoA, and 0.5 μCi [L-methyl-^{3}H]carnitine) was added to the preincubated samples to a 100-μL final volume. The mixture was incubated at 30°C for 20 minutes, and the reaction was stopped by the addition of 1.2 mmol/L HCl. ^{3}H-Palmitoylcarnitine formed during the reaction was extracted from the mixture with water-saturated butanol and measured using a Packard 1900R scintillation counter (Perkin Elmer).

For the mitochondrial glycerol-3-phosphate dehydrogenase (mGPDH) enzyme assay, liver tissue was homogenized in SET buffer; and the homogenate was centrifuged at 800*g* for 10 minutes at 4°C. The nuclear pellet was discarded, and the supernatant was transferred into new tubes and centrifuged at 10 000*g* to precipitate the mitochondria. The mitochondrial pellet was rinsed twice in SET buffer and finally resuspended in fresh SET buffer, aliquoted, and stored at −80° until analyzed. Liver mGPDH

activity was measured spectrophotometrically following the reduction of 2,6 dichlorophenol indophenol at 600 nm [43] in an assay mixture consisting of 50 mmol/L KPO_4 buffer (pH 7.5), 0.1 mmol/L EDTA, 50 mmol/L glycerol-3-phosphate, 1.66 mg/mL 2,6-dichlorophenol indophenol, 1.0 mmol/L KCN, 0.3 mg/mL phenazine methosulfate, and mitochondrial suspension, and calculated using the extinction coefficient 19.1 cm^2 mol^{-1}.

2.6. Determination of mitochondrial biogenesis and aerobic capacity

Mitochondrial biogenesis was assessed by measuring mtDNA copy number using a protocol similar to that described by Niklas et al [44]. The quantity of the mitochondrially encoded gene cytochrome b (Cytb) relative to that of the stable nuclear-encoded gene 18S ribosomal RNA (rRNA) was measured via multiplexed TaqMan-based PCR. Total DNA was isolated from the tissues using a modification of the spin-column protocol from the DNeasy Blood and Tissue Kit. The quantity and quality of DNA were determined spectrophotometrically, and the DNA was stored at 4°C until used.

For the TaqMan primer/probe sets, the 18S rRNA set was an inventoried endogenous control. The Cytb set was custom-designed from a sequence submitted to the Custom TaqMan Gene Expression Assay Service per their recommendations [45]. Briefly, the mitochondrial Cytb sequence obtained from the National Center for Biotechnology Information database was subjected to Basic Localized Alignment Search Tool analyses. The selected target sequence was checked to identify and mask repeats with RepeatMasker [46] and polymorphisms with the National Center for Biotechnology Information dbSNP application. Several preferred probe sites were chosen, and a 549 nucleotide sequence was submitted to Applied Biosystems via their File Builder 3.1 software for primer/probe design. The sequences for the Cytb primer/probe sets were as follows: forward primer, GACCTACTAGGAGACCCA-GACAATT; reverse primer, GCTACGACTCCTCC-TAGTTTGTT; and probe, TCTACGCTCCATTCCC.

Mitochondrial aerobic capacity in AT, liver, and skeletal muscle was determined by measuring the activity of the mitochondrial matrix enzyme citrate synthase as described by Kirby et al [47]. The enzyme assay measured the formation of 5-thio-2-nitrobenzoate at 412 nm in an assay mixture consisting of 100 mmol/L Tris-HCl, pH 8.0, 100 μmol/L 5,5′-dithiobis(2-nitrobenzoic acid), 50 μmol/L acetyl-CoA, 0.1% SDS, 250 μmol/L oxaloacetate, and 50 μg of protein.

2.7. Data analysis

All data are expressed as means ± SEM and were analyzed by paired *t* test using Sigma Stat (Systat, San Jose, CA). A P value ≤ .05 was considered statistically significant.

3. Results

3.1. Adiposity and serum parameters in CF and MR rats

Table 1 shows the effects of MR on AT weights and serum parameters. As previously reported [3], AT weight expressed as a percentage of body weight was significantly reduced by 50% in all depots, corresponding to a significant 3-fold reduction in serum leptin and a 2-fold induction in serum adiponectin. Serum levels of glucose, insulin, insulin-like growth factor–1 (IGF-1), triglycerides, and cholesterol were also reduced by MR; but levels of free fatty acids remained unchanged. Methionine restriction also reduced serum levels of thyroxine, whereas it increased serum levels of triiodothyronine (T3) as reported by Malloy et al [3]. As in a number of rodent models of AR and increased life span, MR rats are smaller in size than CF rats, corresponding with a decrease in organ size attributed to the decrease in IGF-1. When expressed as a percentage of total body weight, however, the reduction in the weights of organs such as liver and kidney is not as pronounced as that observed in ATs (Table 1). These results clearly show the dramatic effects of MR on AT compared with other tissues.

3.2. Gene expression in inguinal AT from CF and MR rats

To determine whether MR influences mitochondrial biogenesis, the expression of genes controlling this process was evaluated in inguinal AT by qPCR. Fold-changes in inguinal AT gene expression induced by MR relative to the gene expression observed in CF rats are shown in Table 2. Methionine restriction was found to induce the expression

Table 1
Tissue weights as a percentage of body weight, serum parameters, and adiposity markers in CF and MR rats

Parameter	CF	MR
Body weight	350 ± 12	191 ± 3*
Fat as percentage of body weight		
Inguinal	3.5 ± 0.8	1.8 ± 0.1*
Epididymal	2.1 ± 0.6	1.2 ± 0.4*
Retroperitoneal	2.0 ± 0.6	1.1 ± 0.3*
Organs as percentage of body weight		
Liver	3.74 ± 0.1	3.46 ± 0.1*
Kidney	0.34 ± 0.004	0.38 ± 0.1*
Serum parameters		
Triglycerides (mg/dL)	103 ± 7	34 ± 3*
Cholesterol (mg/dL)	46 ± 1	38 ± 1*
Free fatty acids (mEq/L)	15 ± 1	16 ± 2
Glucose (mg/dL)	186 ± 8	161 ± 3*
Hormones		
Insulin (ng/mL)	1.14 ± 0.09	0.43 ± 0.04*
IGF-1 (μg/mL)	1.34 ± 0.46	0.57 ± 0.02*
Adiponectin (μg/mL)	4.94 ± 0.51	12.74 ± 0.29*
Leptin (pg/mL)	10.86 ± 1.35	2.41 ± 0.33*
Thyroxine (μg/dL)	6.21 ± 0.13	5.13 ± 0.11*
T3 (ng/dL)	152.00 ± 6.28	352.83 ± 14.15*

Values are expressed as the mean ± SEM of 7 samples and analyzed by paired *t* test.

* $P \leq .050$.

Table 2
Gene and protein expression levels in inguinal AT from CF and MR F344 rats

Gene	Fold-change			Protein	Fold-change		
	CF	MR	*P* value		CF	MR	*P* value
Ppargc1a	1.00 ± 0.12	3.41 ± 0.37	<.001*	PGC1α	1.00 ± 0.22	1.06 ± 0.28	0.883
Ppargc1b	1.00 ± 0.09	1.53 ± 0.11	.003*	–	–	–	–
Nrf1	1.00 ± 0.06	1.22 ± 0.07	.051	–	–	–	–
Nrf2	1.00 ± 0.07	1.05 ± 0.07	.083	–	–	–	–
Tfam	1.00 ± 0.04	1.38 ± 0.10	.005*	–	–	–	–
Cox4i1	1.00 ± 0.05	1.63 ± 0.07	<.001*	COX4	1.00 ± 0.15	1.52 ± 0.13	.033*
Ucp1	1.00 ± 0.36	29.72 ± 7.42	<.001*	UCP1	1.00 ± 0.14	1.27 ± 0.46	.591
Ucp2	1.00 ± 0.16	0.82 ± 0.26	.867	–	–	–	–
Ucp3	1.00 ± 0.19	0.94 ± 0.23	.571	–	–	–	–
Esrra	1.00 ± 0.10	1.12 ± 0.17	.573	–	–	–	–
Esrrg	1.00 ± 0.08	1.08 ± 0.10	.549	–	–	–	–
Ppara	1.00 ± 0.09	1.43 ± 0.12	.014*	PPARα	1.00 ± 0.22	1.29 ± 0.15	.307
Ppard	1.00 ± 0.12	1.00 ± 0.22	.366	–	–	–	–
Pparg	1.00 ± 0.19	1.61 ± 0.30	.092	PPARγ	1.00 ± 1.00	5.62 ± 1.58	.063
Fabp4	1.00 ± 0.10	1.86 ± 0.08	<.001*	FABP4	1.00 ± 0.26	2.11 ± 0.31	.025*
Cpt1a	1.00 ± 0.12	3.70 ± 0.38	<.001*	CPT1	1.00 ± 0.10	2.13 ± 0.25	.002*
Acadm	1.00 ± 0.08	1.34 ± 0.06	.010*	MCAD	1.00 ± 0.11	1.58 ± 0.34	.143
Scd1	1.00 ± 0.09	4.25 ± 0.35	.001*	SCD1	1.00 ± 0.41	15.33 ± 5.29	.008*
Pdk4	1.00 ± 0.20	1.03 ± 0.31	.945	–	–	–	–
Adra2a	1.00 ± 0.19	0.47 ± 0.09	.069	–	–	–	–
Adrb3	1.00 ± 0.15	2.25 ± 0.29	.004*	Adrβ3	1.00 ± 0.09	1.57 ± 0.03	<.001*

Gene expression was assessed by TaqMan-based qPCR. Protein levels were determined by Western blotting or enzyme analysis. Relative protein content in Western blots was normalized with β-actin. The CPT1 activity was analyzed enzymatically as described in "Materials and methods." Results are expressed as the means ± SEM of 7 samples per treatment group and analyzed by paired *t* test.

* $P < .05$.

of *Ppargc1a* and *Ppargc1b* by approximately 3-fold and 1.5-fold, respectively. As PGC1α triggers mitochondrial biogenesis through the activation of NRFs and the transcriptional up-regulation of *Tfam*, levels of *Nrf1*, *Nrf2*, and *Tfam* mRNA were also measured. No difference in *Nrf1* and *Nrf2* gene expression was observed in inguinal AT from CF and MR rats, but *Tfam* expression was significantly induced 1.38-fold.

Up-regulation of mitochondrial oxidative and uncoupling capacity is a reported PGC1α effect [18]; therefore, the expression of *Cox4* and *Ucp1* was examined. *Cox4* and *Ucp1* mRNA levels were significantly increased 1.6- and 29-fold, respectively (Table 2), suggesting the potential induction of both AT mitochondrial oxidative and uncoupling capacity. In contrast to MR's effects on *Ucp1* gene expression in inguinal AT, no transcriptional changes were observed for *Ucp2* and *Ucp3*.

Mitochondrial biogenesis and oxidative capacity also involve the activation of nuclear receptors followed by the up-regulation of their target genes [19]; therefore, the effects of MR on the expression of nuclear receptors were examined. Methionine restriction caused no significant changes in the transcription of *Esrrs* and *Ppars*, except for *Ppara*, which was significantly induced 1.4-fold.

Methionine restriction's effects on ERR and PPAR target genes were also examined. Although *Pparg* mRNA levels were not significantly different between inguinal AT from CF and MR rats, the expression of *Fabp4*, a PPARγ target gene, was significantly induced 1.8-fold. The expression of *Cpt1a* and *Acadm*, genes involved in fatty acid oxidation and controlled by the interaction of PGC1α with PPARα and ERRs, respectively [48-51], was significantly induced by MR. Methionine restriction also increased the expression of *Scd1*, a PPARδ target gene; but had no effect on *Pdk4* mRNA levels.

Because AT oxidative capacity can be controlled by adrenergic stimulation, which also up-regulates *Ppargc1a* expression [52], MR's effects on adrenergic receptor gene expression were examined. A trend toward a decrease in *Adra2a* gene expression and a significant increase in *Adrb3* gene expression was observed in inguinal AT from MR rats, suggesting enhanced tissue sensitivity to Adrβ3 agonists. These results correspond with our report showing an increased response of MR rat adipocytes to isoproterenol [5].

3.3. Comparison of AT gene expression profiles

Adipose tissues are functionally heterogeneous with respect to their endocrine function and lipid storage/buffering capacity (reviewed by Sharma and Staels [31]) as a result of differences in gene and protein expression [53,54]. The gene expression profile induced in inguinal AT by MR was therefore compared with gene expression profiles observed in epididymal and retroperitoneal ATs (Fig. S1). Although MR induced similar gene expression changes in all ATs, its effects were more pronounced in inguinal and epididymal fat. The gene expression signature observed in epididymal AT from MR rats was almost identical to that of

inguinal fat, except for differences in *Ppard*, *Adrb3*, and *Cpt1a* expression levels. In contrast to inguinal and epididymal fat, *Nrf2* expression was significantly increased in retroperitoneal AT.

3.4. Confirmation of gene expression changes induced by MR in inguinal AT

The translation of mRNA into proteins may be influenced by antisense-mediated mRNA decay or microRNAs (reviewed by Shyu et al [55] and Zhang [56]). To evaluate the significance of gene expression changes induced by MR, protein or enzyme activity levels for some genes were examined in inguinal AT (Table 2). Methionine restriction caused no changes in PGC1α, PPARα, and PPARγ protein levels. The COX4 protein levels were significantly increased 1.5-fold; but, surprisingly, no differences in UCP1 protein levels were evident between the 2 treatment groups despite the dramatic 29-fold mRNA induction. As in the qPCR studies, FABP4 protein levels were significantly increased 2-fold. Because of our inability to measure CPT1 protein levels by Western blotting, CPT1 enzyme activity was assayed, showing a 2-fold increase in MR rats. The MCAD protein levels were induced by MR but were not significantly different from those levels observed in inguinal AT from CF rats; however, protein levels for SCD1 were significantly increased 15-fold by MR. Finally, in agreement with the previously reported increased sensitivity of MR rat adipocytes to the Adrβ3 agonist isoproterenol, a 1.5-fold induction in Adrβ3 protein level was observed in inguinal AT from MR rats.

3.5. Gene and protein expression in liver and skeletal muscle from CF and MR rats

In addition to AT, liver and skeletal muscle play important roles in lipid metabolism; thus, gene expression analyses were also conducted in these tissues (Table 3). Methionine restriction induced the expression of *Ppargc1s*, *Nrf2*, *Esrrs*, *Ppars*, and their target genes in liver and muscle (Tables 3A and B, respectively). In liver tissue, *Ppara* gene expression was significantly induced by MR; but no change in the gene expression of acyl-CoA oxidase 2 (*Acox2*), a PPARα target gene in liver, was observed. Unlike *Acox2*, the PPARα target gene *Cpt1a* was significantly up-regulated in liver from MR rats. MR induced the expression of liver *Gpd2*, recently reported to participate in fatty acid oxidation [57]. Methionine restriction also significantly reduced the expression of *Fabp1* and *Scd1*, genes that are translated into enzymes involved in lipid storage and monounsaturated fatty acid synthesis, respectively.

In skeletal muscle, in addition to up-regulating the expression of all coactivators and nuclear receptors examined, MR significantly induced the expression of the PPARδ target genes *Cpt1b*, *Scd1*, *Pdk4*, and *Ucp3* (Table 3B), all of which are associated with the transformation of glycolytic (type II) to lipid oxidizing (type I) myofibers [58].

Western blot and enzyme analyses were also conducted to confirm the gene expression changes observed in liver and skeletal muscle. Although mRNA levels were up-regulated by MR, no changes in PGC1, ERRα, and PPARα protein levels were observed in liver tissue (Table 3A). In contrast, PPARγ protein expression was significantly induced more than 2-fold in liver. No significant changes in COX4 protein levels or CPT1 enzyme activity were observed in livers from MR rats. In contrast, MR resulted in a dramatic 100-fold reduction in SCD1 protein levels and a significant 1.3-fold increase in mGPDH activity, in agreement with the gene expression data.

Contrary to the gene expression signature observed in skeletal muscle from MR rats, no significant protein expression changes were observed for PGC1α, PPARs, and their target genes, except for COX4 and UCP3, which were up-regulated 1.5- and 1.8-fold, respectively (Table 3B). The induction of PPARδ target genes has been associated with the transformation of muscle fibers from a glycolytic- to a lipid-oxidizing phenotype, a process involving the increased expression of myoglobin and slow-twitch troponin [58,59]; however, no transformation of skeletal muscle fibers into lipid-oxidative fibers was evident because no differences in myoglobin and slow-twitch troponin protein levels were observed between CF and MR rat skeletal muscles (Table 3B).

3.6. Assessment of mitochondrial biogenesis and aerobic capacity in AT

The PGC1s control mitochondrial biogenesis through the induction of *Nrf*s and *Tfam* expression and activity [60,61]. Considering that MR induced the expression of *Ppargc1s* and *Tfam*, mitochondrial biogenesis was assessed by measuring mtDNA copy number in inguinal AT, liver, and skeletal muscle. A 2-fold increase in mtDNA content was observed in MR rat inguinal AT (Fig. 1A). This is the first study showing changes in inguinal AT mtDNA content in response to physiologic adaptations induced by MR. In contrast to inguinal AT, no changes in mtDNA copy number were observed in liver (Fig. 1B) and in skeletal muscle (Fig. 1C).

Citrate synthase is the first enzyme in the Krebs cycle that catalyzes the formation of citric acid from CoA and oxaloacetic acid and is considered a marker of mitochondrial aerobic activity and mitochondrial mass [7]. A 2-fold increase in mitochondrial citrate synthase activity was observed in inguinal AT (Fig. 1D), suggesting increased mitochondrial aerobic capacity in this tissue. Significant inductions in citrate synthase activity by MR were also observed in liver (Fig. 1E) and skeletal muscle (Fig. 1F).

Because visceral AT has been reported to play an important role in obesity-related diseases and aging [73], studies on mitochondrial biogenesis and aerobic capacity were extended to epididymal AT, a visceral fat depot. Methionine restriction caused no significant changes in

Table 3
Gene and protein expression levels in liver and skeletal muscle from CF and MR F344 rats

Gene	Fold-change			Protein	Fold-change		
	CF	MR	*P value*		CF	MR	*P value*
A. Liver							
Ppargc1a	1.00 ± 0.13	2.36 ± 0.15	<.001*	PGC1α	1.00 ± 0.09	1.15 ± 0.16	0.429
Ppargc1b	1.00 ± 0.04	1.35 ± 0.06	<.001*	–	–	–	–
Nrf1	1.00 ± 0.04	1.69 ± 0.07	<.001*	–	–	–	–
Nrf2	1.00 ± 0.01	1.25 ± 0.05	<.001*	–	–	–	–
Tfam	1.00 ± 0.03	1.60 ± 0.07	<.001*	–	–	–	–
Cox4i1	1.00 ± 0.02	1.52 ± 0.06	<.001*	COX4	1.00 ± 0.06	1.06 ± 0.09	0.608
Ucp2	1.00 ± 0.03	1.05 ± 0.05	.420	–	–	–	–
Esrra	1.00 ± 0.02	2.03 ± 0.08	<.001*	ERRα	1.00 ± 0.27	1.24 ± 0.60	1.000
Esrrg	1.00 ± 0.09	0.89 ± 0.09	.420	–	–	–	–
Ppara	1.00 ± 0.06	1.51 ± 0.09	<.001*	PPARα	1.00 ± 0.14	0.97 ± 0.18	0.887
Ppard	1.00 ± 0.18	0.82 ± 0.04	.710	–	–	–	–
Pparg	1.00 ± 0.11	1.64 ± 0.17	.012*	PPARγ	1.00 ± 0.23	2.64 ± 0.30	0.019*
Acox2	1.00 ± 0.05	1.02 ± 0.04	.797	–	–	–	–
Fabp1	1.00 ± 0.07	0.59 ± 0.02	<.001*	–	–	–	–
Cpt1a	1.00 ± 0.06	1.92 ± 0.15	<.001*	CPT1	1.00 ± 0.07	1.26 ± 0.17	0.188
Acadm	1.00 ± 0.03	0.98 ± 0.04	.728	–	–	–	–
Scd1	1.00 ± 0.10	0.09 ± 0.03	<.001*	SCD1	1.00 ± 0.25	0.01 ± 0.01	0.002*
Pdk4	1.00 ± 0.08	1.02 ± 0.15	.912	–	–	–	–
Gpd2	1.00 ± 0.09	1.69 ± 0.09	<.001*	mGPDH	1.00 ± 0.04	1.30 ± 0.11	0.032*
B. Skeletal muscle							
Ppargc1a	1.00 ± 0.11	1.41 ± 0.08	.013*	PGC1α	1.00 ± 0.09	0.79 ± 0.06	0.073
Ppargc1b	1.00 ± 0.11	1.26 ± 0.12	.134	–	–	–	–
Nrf1	1.00 ± 0.08	1.34 ± 0.09	.014*	–	–	–	–
Nrf2	1.00 ± 0.07	1.30 ± 0.06	.009*	–	–	–	–
Tfam	1.00 ± 0.08	1.36 ± 0.08	.011*	–	–	–	–
Cox4i1	1.00 ± 0.09	1.32 ± 0.11	.047*	COX4	1.00 ± 0.14	1.57 ± 0.22	0.049*
Ucp2	1.00 ± 0.07	1.13 ± 0.04	.120	–	–	–	–
Ucp3	1.00 ± 0.26	1.77 ± 0.15	.022*	UCP3	1.00 ± 0.27	1.87 ± 0.11	0.017*
Esrra	1.00 ± 0.08	1.40 ± 0.10	.010*	–	–	–	–
Esrrg	1.00 ± 0.20	2.21 ± 0.40	.027*	–	–	–	–
Ppara	1.00 ± 0.11	1.50 ± 0.14	.016*	–	–	–	–
Ppard	1.00 ± 0.08	1.38 ± 0.06	.003*	PPARδ	1.00 ± 0.15	1.39 ± 0.15	0.091
Pparg	1.00 ± 0.04	1.54 ± 0.13	.004*	PPARγ	1.00 ± 0.35	0.51 ± 0.11	0.208
Cpt1b	1.00 ± 0.07	1.51 ± 0.10	.001*	CPT1	1.00 ± 0.14	0.41 ± 0.07	0.003*
Acadm	1.00 ± 0.13	1.61 ± 0.14	.009*	MCAD	1.00 ± 0.05	1.19 ± 0.22	0.710
Scd1	1.00 ± 0.27	4.03 ± 1.43	.071	SCD1	1.00 ± 0.13	0.96 ± 0.12	0.823
Pdk4	1.00 ± 0.18	2.97 ± 0.14	<.001*	PDK4	1.00 ± 0.11	0.96 ± 0.05	0.719
Gpd2	1.00 ± 0.07	1.04 ± 0.11	.794	–	–	–	–
				Myoglobin	1.00 ± 0.12	1.06 ± 0.07	0.689
				Troponin	1.00 ± 0.09	0.96 ± 0.09	0.755

Gene expression was assessed by TaqMan-based qPCR. Protein levels were determined by Western blotting or enzyme analysis. Relative protein content was normalized with β-actin in liver and α-tubulin in skeletal muscle Western blots. The CPT1 and mGPDH activities were analyzed as described in "Materials and methods." Results are expressed as the means ± SEM of 7 samples per treatment group and analyzed by paired *t* test.

* $P < .05$.

mtDNA content in this tissue, although citrate synthase activity was significantly enhanced by this dietary regimen (Fig. 2).

4. Discussion

Methionine restriction induced tissue-specific changes in gene and protein expression in WAT, liver, and skeletal muscle. In inguinal (subcutaneous) AT, MR up-regulated the expression of *Ppargc1s*, *Ppars*, and their known target genes; mtDNA content; and mitochondrial citrate synthase activity, suggesting the onset of mitochondrial biogenesis in this tissue. In contrast, mtDNA content was not changed in liver, skeletal muscle, and epididymal (visceral) AT from MR rats despite the fact that mitochondrial aerobic capacity was enhanced in these tissues. An important finding in liver was the dramatic decrease in *Scd1* gene and protein expression and a modest increase in *Gpd2* gene expression and enzyme activity, suggesting a potential shift from fatty acid synthesis to fatty acid oxidation. In skeletal muscle, MR increased *Ucp3* gene and protein expression, which participates in the facilitation of fatty acid oxidation. Collectively, these tissue-specific responses could lead to

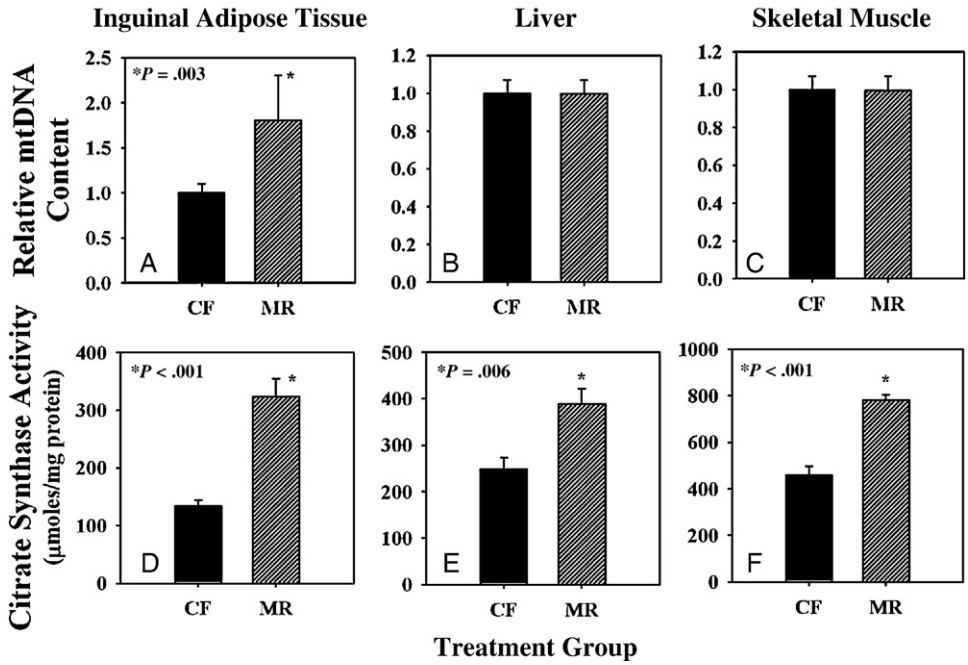

Fig. 1. Assessment of mitochondrial biogenesis and oxidative capacity in inguinal AT, liver, and skeletal muscle. Mitochondrial DNA copy number was determined by the amplification of mitochondrially encoded Cytb DNA relative to the nuclear-encoded 18S rRNA gene. Mitochondrial oxidative capacity was assessed by measuring citrate synthase activity. Values are expressed as the means ± SEM and analyzed by paired *t* test.

increased mitochondrial function and possibly the induction of fatty acid oxidation, thereby contributing to the AR and insulin sensitivity observed in MR rats.

The mechanism behind the MR effects on inguinal AT has not been elucidated, but it could involve adrenergic stimulation. Methionine restriction was shown to significantly up-regulate *Adrb3* mRNA and protein levels in inguinal AT, corresponding with the reported increased sensitivity of mature adipocytes from MR rats to isoproterenol [5]. Chronic activation of Adrβ3 triggers mitochondrial biogenesis and fatty acid oxidation in WAT and correlates with the increased expression of PPARα and its target genes [37,52,62]. When *Ppar*α is deleted, the observed Adrβ3 effects are compromised, implicating the involvement of PPARα in adrenergic-mediated induction of AT mitochondrial biogenesis and oxidative capacity [37].

Adrenergic stimulation also increases serum levels of T3, which was shown to trigger *Ppargc1*α gene expression and a 2-fold increase in *Ucp1* mRNA levels [63]. During chronic adrenergic stimulation, the up-regulation of *Ucp1* gene expression by T3 is further increased to 20-fold (reviewed by Silva and Bianco [63]). In this study, *Ucp1* gene expression in inguinal and epididymal fat was increased 29-fold; and as MR rats have high T3 serum levels [3], there is the possibility that some of the observed MR effects on AT may be mediated by a synergistic action of activated adrenergic receptors and thyroid hormone signaling.

Another potential mechanism behind the MR effects could involve the activation of PPARs. Adipocytes from MR rats display increased lipolysis [5], and fatty acids released from this process are PPAR agonists. In this study, activation of PPARs was suggested by the up-regulation of some of their target genes. The PPARγ activation by pioglitazone was reported to increase mtDNA copy number and the expression of mitochondrial biogenesis transcription factors,

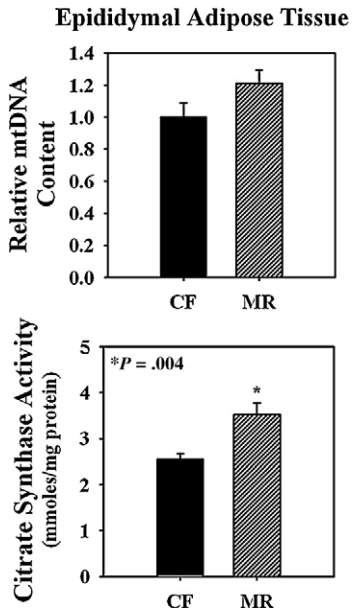

Fig. 2. Assessment of mitochondrial biogenesis and oxidative capacity in epididymal AT. Mitochondrial DNA copy number and citrate synthase activity were determined as described previously. Values are expressed as the means ± SEM of 7 samples per treatment group and analyzed by paired *t* test.

including *Ppargc1α* and *Tfam*, in WAT of obese and insulin-resistant humans and mice [13,15]. The PPARγ activation also up-regulates genes involved in fatty acid oxidation such as *Pparα*, *Cpt1*, and *Acadm* [13,15].

Methionine restriction significantly increased *Ucp1* gene expression in inguinal AT. Uncoupling protein 1 induces a proton leak in the inner mitochondrial membrane leading to the uncoupling of fuel oxidation and adenosine triphosphate synthesis causing the release of energy in the form of heat (thermogenesis). However, an uncoupling effect mediated by UCP1 in inguinal AT from MR rats is unlikely because no changes in UCP1 protein levels were observed. The decreased adiposity in MR rats may in part be mediated by enhanced fuel oxidation or by an UCP1-independent thermogenic effect. In fact, in inguinal AT, MR increased the gene expression and activity of CPT1, the rate-limiting enzyme in mitochondrial fatty acid oxidation.

To gain further insight into other potential mechanism(s) leading to AR in MR rats, the gene expression analysis was extended to liver and skeletal muscle, considering that these 2 tissues play important roles in the maintenance of lipid homeostasis. Methionine restriction induced gene expression profiles in liver and skeletal muscle similar to those observed in ATs; however, no significant changes in protein levels or enzyme activities were observed in these tissues.

Although MR did not increase mitochondrial biogenesis in liver, mitochondrial aerobic capacity was enhanced. An interesting finding in liver tissue from MR rats was the induction of *Gpd2* mRNA and its enzyme activity levels. Mitochondrial glycerol-3-phosphate dehydrogenase is involved in the dihydroacetone/glycerol-3-phosphate shuttle through which reduced nicotinamide adenine dinucleotide generated in the cytoplasm is transferred to coenzyme Q in the mitochondrial electron transport chain, bypassing complex I [64]. This reaction is exothermic, driven by the difference in free energy of nicotinamide adenine dinucleotide in the cytosol and reduced flavin adenine dinucleotide in the mitochondria [64]. Because of its exothermic nature, the energy released from this reaction could contribute to the overall energy expenditure previously reported in MR rats. Mitochondrial glycerol-3-phosphate dehydrogenase is also an indicator of hepatic fatty acid oxidation in rat strains resistant to age- and diet-induced obesity [57]. It is therefore likely that the increased aerobic activity observed in MR rat liver mitochondria could be associated with increased fatty acid oxidation in this tissue. It is also important to mention that complex I in the mitochondrial electron transport chain is a site where reactive oxygen species are generated and, thus, the transfer of reducing equivalents bypassing complex I reduces oxidative damage despite increases in mitochondrial oxidative capacity.

Another important finding in liver from MR rats was the dramatic decrease in *Scd1* mRNA and protein expression levels. Stearoyl-CoA desaturase 1 is involved in the de novo synthesis of monounsaturated fatty acids contributing to the formation of phospholipids, triglycerides, cholesterol, and other lipid molecules in response to high-carbohydrate or high-fat feeding; and its inhibition impairs high-fat– or high-carbohydrate–induced obesity, steatohepatitis, and insulin resistance [65]. Stearoyl-CoA desaturase 1 has also been implicated in fatty acid partitioning by promoting fatty acid synthesis and reducing fatty acid oxidation [65]. Although SCD1-deficient mice exhibit increased lipid oxidation and energy expenditure through thermogenic pathways eliciting resistance to obesity [65], hepatic SCD1 deficiency alone is insufficient to induce a hypermetabolic phenotype [66]. Ablation of liver-specific SCD1 still protects against high-carbohydrate–induced obesity and steatosis [67]; therefore, SCD1 inhibition in the liver by MR could be contributing to the AR and insulin sensitivity reported in this animal model [3].

Although liver SCD1 protein levels were dramatically reduced in MR rats, these were significantly induced in inguinal AT. Stearoyl-CoA desaturase 1 in AT produces the lipokine C16:1n7-palmitoleate, which has been demonstrated to inhibit *Scd1* gene expression and activity in liver from aP2- and mal1-deficient mice, making them resistant to hepatosteatosis [68]. It is therefore possible that the reduction of hepatic SCD1 protein expression in liver from MR rats could be controlled by the release of C16:1n7-palmitoleate from inguinal AT, but this requires further investigation.

As in the liver, mitochondrial biogenesis was not changed in skeletal muscle by MR; but mitochondrial aerobic activity was still induced. Only UCP3 and COX4 protein levels were significantly increased in skeletal muscle by MR. Skeletal muscle *Ucp3* gene expression is tightly regulated by metabolic signals related to fatty acid availability and thyroid hormone levels [69]; thus, increased T3 levels in MR rats [3] could be associated with the transcriptional regulation of this gene. Mice overexpressing *Ucp3* show marked elevations in metabolic rates and lipid oxidation, suggesting that UCP3 drives a shift in substrate utilization from carbohydrates to lipid during fasting [70], thereby reducing adiposity [71]. Although UCP3 has no direct involvement in the fatty acid oxidative pathway, increased fatty acid oxidation by UCP3 was recently reported to be driven by the reduction of mitochondrial oxidative stress [72]. Increased UCP3 protein levels in MR rat skeletal muscle could be up-regulating fatty acid oxidation in this tissue, which could explain the observed effects of MR on citrate synthase activity.

Methionine restriction induced similar gene expression changes in inguinal (subcutaneous) and epididymal (visceral) ATs, but this dietary regimen failed to increase mtDNA content in epididymal fat. Subcutaneous and visceral fat depots are anatomically, metabolically, and physiologically different [73], which could explain their specific responses to MR. Despite the differences in mitochondrial biogenesis, mitochondrial function was up-regulated in both AT types. Induction of mitochondrial biogenesis and function stimulates adiponectin synthesis in cultured adipocytes, whereas

the impairment of mitochondrial function exerts the opposite effect [74]. It is therefore likely that induction of mitochondrial content and/or function by MR may be associated with increased serum adiponectin in MR rats, which correlates with insulin sensitivity and lean body mass [74].

It is concluded that MR triggers an array of tissue-specific adaptive responses that collectively contribute to insulin sensitivity and AR. In ATs, MR stimulated mitochondrial biogenesis and/or aerobic capacity, which correlates with increased serum adiponectin, an anti-inflammatory adipokine associated with insulin sensitivity and lean phenotypes. In liver and skeletal muscle, MR mediated the up-regulation of genes and proteins that are involved in metabolic adaptations that ultimately increase fatty acid oxidation. In addition to the lipid futile cycle observed in WAT of MR rats [5], MR also induces another futile cycle: the dihydroacetone/glycerol-3-phosphate shuttle in the liver. Whether these mechanisms are controlled by the activation of PPARs, adrenergic stimulation, and/or the induction of T3 signaling in MR rats is currently under investigation.

Acknowledgment

We thank Heidi Seymour for her outstanding assistance with the animal husbandry, and blood and tissue collections.

Appendix A. Supplementary data

Supplementary data associated with this article can be found, in the online version, at doi:10.1016/j.metabol.2009.10.023.

References

[1] Orentreich N, Matias JR, DeFelice A, Zimmerman JA. Low methionine ingestion by rats extends life span. J Nutr 1993;123:269-74.
[2] Miller RA, Buehner G, Chang Y, Harper JM, Sigler R, Smith-Wheelock M. Methionine-deficient diet extends mouse lifespan, slows immune and lens aging, alters glucose, T4, IGF-1 and insulin levels, and increases hepatocyte MIF levels and stress resistance. Aging Cell 2005;4:119-25.
[3] Malloy V, Krajcik R, Bailey S, Hristopoulos G, Plummer J, Orentreich N. Methionine restriction decreases visceral fat mass and preserves insulin action in aging male Fischer 344 rats independent of energy restriction. Aging Cell 2006;5:305-14.
[4] Zimmerman JA, Malloy V, Krajcik R, Orentreich N. Nutritional control of aging. Exp Gerontol 2003;38:47-52.
[5] Perrone CE, Mattocks DAL, Hristopoulos G, Plummer JD, Krajcik RA, Orentreich N. Methionine restriction effects on 11β-HSD1 activity and lipogenic/lipolytic balance in F344 rat adipose tissue. J Lipid Res 2008;49:12-23.
[6] Toh SY, Gong J, Du G, Li JZ, Yang S, Ye J, et al. Up-regulation of mitochondrial activity and acquirement of brown adipose tissue-like property in white adipose tissue of fsp27 deficient mice. PLOS One 2008;3:e2890.
[7] Katic M, Kennedy AR, Leikin I, Norris A, McGettrick A, Gesta S, et al. Mitochondrial gene expression and increased oxidative metabolism: role in increased lifespan of fat-specific insulin receptor knock-out mice. Aging Cell 2007;6:827-39.
[8] Shadel GS. Expression and maintenance of mitochondrial DNA: new insights into human disease pathology. Am J Pathol 2008;172:1445-56.
[9] Maassen JA. Mitochondrial dysfunction in adipocytes: the culprit in type 2 diabetes? Diabetologia 2006;49:619-20.
[10] Petersen KF, Dufour S, Befroy D, Garcia R, Shulman GI. Impaired mitochondrial activity in the insulin-resistance offspring of patients with type 2 diabetes. N Engl J Med 2004;350:664-71.
[11] Turner N, Heilbronn LK. Is mitochondrial dysfunction a cause of insulin resistance? Trends Endocrinol Metab 2008;19:324-30.
[12] Rogge MM. The role of impaired mitochondrial lipid oxidation in obesity. Biol Res Nurs 2009;10:356-73.
[13] Bogacka I, Xie H, Bray GA, Smith SR. Pioglitazone induces mitochondrial biogenesis in human subcutaneous adipose tissue in vivo. Diabetes 2005;54:1392-9.
[14] Choo HJ, Kim JH, Kwon OB, Lee CS, Mun JY, Hann SS, et al. Mitochondria are impaired in the adipocytes of type 2 diabetic mice. Diabetologia 2006;49:784-91.
[15] Rong JX, Qiu Y, Hansen MK, Zhu L, Zhang V, Xie M, et al. Adipose mitochondrial biogenesis is suppressed in *db*/*db* and high-fat diet-fed mice and improved by rosiglitazone. Diabetes 2007;56:1751-60.
[16] Semple RK, Crowley VC, Sewter CP, Laudes M, Christodoulides C, Considine RV, et al. Expression of the thermogenic nuclear hormone receptor coactivator PGC-1alpha is reduced in the adipose tissue of morbidly obese subjects. Int J Obes Relat Metab Disord 2004;28:176-9.
[17] Bogacka I, Ukropcova B, McNeil M, Gimble JM, Smith SR. Structural and functional consequences of mitochondrial biogenesis in human adipocytes in vitro. J Clin Endocrinol Metab 2005;90:6650-6.
[18] Puigserver P, Wu Z, Park CW, Grace R, Wright M, Spiegelman BM. A cold-inducible coactivator of nuclear receptors linked to adaptive thermogenesis. Cell 1998;92:829-39.
[19] Puigserver P, Spiegelman BM. Peroxisome proliferator-activated receptor-γ coactivator 1α (PGC-1α): transcriptional coactivator and metabolic regulator. Endocrine Rev 2007;24:78-90.
[20] St-Pierre J, Lin J, Krauss S, Tarr PT, Yang R, Newgard CB, et al. Bioenergetic analysis of peroxisome proliferator-activated receptor gamma coactivators 1alpha and 1beta (PGC-1alpha and PGC-1beta) in muscle cells. J Biol Chem 2003;278:26597-603.
[21] Uldry M, Yang W, St-Pierre J, Lin J, Seale P, Spiegelman BM. Complementary action of the PGC-1 coactivators in mitochondrial biogenesis and brown fat differentiation. Cell Metab 2006;3:333-41.
[22] Kamei Y, Ohizumi H, Fujitani Y, Nemoto T, Tanaka T, Takahashi N, et al. PPARγ coactivator 1β/ERR ligand 1 is an ERR protein ligand, whose expression induces a high-energy expenditure and antagonizes obesity. Proc Natl Acad Sci U S A 2003;100:12378-83.
[23] Handschin C, Spiegelman BM. Peroxisome proliferator-activated receptor gamma coactivator 1 coactivators, energy homeostasis, and metabolism. Endocr Rev 2006;27:728-35.
[24] Haluzík MM, Haluzík M. PPAR-α and insulin sensitivity. Physiol Res 2006;55:115-22.
[25] Grimaldi PA. Peroxisome proliferator-activated receptors as sensors of fatty acids and derivatives. Cell Mol Life Sci 2007;64:2459-64.
[26] Clayton DA. Replication and transcription of vertebrate mitochondrial DNA. Ann Rev Cell Biol 1991;7:453-78.
[27] Lin J, Handschin C, Spiegelman BM. Metabolic control through the PGC-1 family of transcription coactivators. Cell Metabolism 2005;1:361-70.
[28] Scarpulla RC. Nuclear activators and coactivators in mammalian mitochondrial biogenesis. Biochem Biophys Acta 2002;1576:1-14.
[29] Sladek R, Bader J-A, Giguère V. The orphan nuclear-related receptor α is a transcriptional regulator of the human medium-chain acyl coenzyme A dehydrogenase gene. Mol Cell Biol 1997;17:5400-9.
[30] Finck BN, Kelly DP. PGC-1 coactivators: inducible regulators of energy metabolism in health and disease. J Clin Invest 2006;116:615-22.

[31] Sharma AM, Staels B. Review: peroxisome proliferator-activated receptor γ and adipose tissue-understanding obesity-related changes in regulation of lipid and glucose metabolism. J Clin Endocrin Metab 2007;92:386-95.
[32] Rosen ED, Walkey CJ, Puigserver P, Spiegelman BM. Transcriptional regulation of adipogenesis. Genes Dev 2000;14:1293-307.
[33] Yamauchi T, Kamon J, Waki H, Murakami K, Motojima K, Komeda K, et al. The mechanisms by which both heterozygous peroxisome proliferator-activated receptor γ (PPARγ) deficiency and PPARγ agonist improve insulin resistance. J Biol Chem 2001;276:41245-54.
[34] Kelly LJ, Vicario PP, Thompson GM, Candelore MR, Doebber TW, Ventre J, et al. Peroxisome proliferator-activated receptors γ and α mediate in vivo regulation of uncoupling protein (UCP-1, UCP-2, UCP-3) gene expression. Endocrinology 1998;139:4920-7.
[35] Fukui Y, Masui S, Osada S, Umesono K, Motojima K. A new thiazolidinedione, NC-2100, which is a weak PPAR-γ activator, exhibits potent antidiabetic effects and induces uncoupling protein 1 in white adipose tissue of KKAy obese mice. Diabetes 2000;49:759-67.
[36] Sell H, Beger JP, Samson P, Castriota G, Lalonde J, Deshaies Y, et al. Peroxisome proliferator-activated receptor γ agonism increases the capacity for sympathetically mediated thermogenesis in lean and ob/ob mice. Endocrinology 2004;145:3925-34.
[37] Li P, Zhu Z, Lu Y, Granneman JG. Metabolic and cellular plasticity in white adipose tissue II: role of peroxisome proliferator-activated receptor–α. Am J Physiol Endocrinol Metab 2007;289:E617-E626.
[38] Richie JP, Leutzinger Y, Parthasarathy S, Malloy V, Orentreich N, Zimmerman JA. Methionine restriction increases blood glutathione and longevity in F344 rats. FASEB J 1994;8:1302-7.
[39] Ström K, Hansson O, Lucas S, Nevsten P, Fernandez C, Klint C, et al. Attainment of brown adipocyte features in white adipocytes of hormone-sensitive lipase null mice. PLOS One 2008;3:e1793.
[40] McGarry JD, Mills SE, Long CS, Foster DW. Observations of the affinity for carnitine, and malonyl-CoA sensitivity, of carnitine palmitoyltransferase I in animal and human tissues. Biochem J 1983; 214:21-8.
[41] Zierz S, Engel AG. Different sites of inhibition of carnitine palmitoyltransferase by malonyl-CoA, and by acetyl-CoA and CoA, in human skeletal muscle. Biochem J 1987;245:205-9.
[42] Kim J-Y, Hickner RC, Cortright RL, Dohm GL, Houmard JA. Lipid oxidation is reduced in obese human skeletal muscle. Am J Physiol Endocrinol Metab 2000;279:E1039-E1044.
[43] Gardner RS. A sensitive colorimetric assay for mitochondrial α-glycerophosphate dehydrogenase. Anal Biochem 1974;59:272-6.
[44] Nicklas J, Brooks EM, Hunter TC, Single R, Branda RF. Assay for relative mitochondrial DNA copy number and the common mitochondrial DNA deletion in the rat. Environ Molec Mutagen 2004;44: 313-20.
[45] Custom TaqMan genomic assays submission guidelines. 2008. Internet communication.
[46] Smit AFA, Hubley R, Green P. RepeatMasker Open-3.0. 1996. Computer program.
[47] Kirby DM, Thorburn DR, Turnbull DM, Taylor RW. Biochemical assays of respiratory chain complex activity. Methods Cell Biol 2007; 80:93-119.
[48] Vega RB, Huss JM, Kelly DP. The coactivator PGC-1 cooperates with peroxisome proliferator-activated receptor alpha in transcriptional control of nuclear genes encoding mitochondrial fatty acid oxidation enzymes. Mol Cell Biol 2000;20:1868-76.
[49] Huss JM, Kopp RP, Kelly DP. Peroxisome proliferator-activated receptor coactivator-1alpha coactivates the cardiac-enriched nuclear receptors estrogen-related receptor-alpha and gamma. Identification of novel leucine-rich interaction motif within PGC-1alpha. J Biol Chem 2002;277:40265-74.
[50] Mootha VK, Handschin C, Arlow D, Xie X, St.Pierre J, Sihag S, et al. Err{alpha} and Gabpa/b specify PGC-1{alpha}–dependent oxidative phosphorylation gene expression that is altered in diabetic muscle. Proc Natl Acad Sci U S A 2004;101:6570-5.
[51] Schreiber SN, Emter R, Hock MB, Knutti D, Cardenas J, Podvinec M, et al. The estrogen-related receptor {alpha} (ERR{alpha}) functions in PPAR{gamma} coactivator 1{alpha} (PGC-1{alpha})–induced mitochondrial biogenesis. Proc Natl Acad Sci U S A 2004;101: 6472-7.
[52] Boss O, Bachman E, Vidal-Puig A, Zhang CY, Peroni O, Lowell BB. Role of the beta(3)-adrenergic receptor and/or a putative beta(4)-adrenergic receptor on the expression of uncoupling proteins and peroxisome proliferator-activated receptor-gamma coactivator–1. Biochem Biophys Res Commun 1999;261:870-6.
[53] Prunet-Marcassus B, Moulin K, Carmona MC, Villarroya F, Penicaud L, Casteilla L. Inverse distribution of uncoupling proteins expression and oxidative capacity in mature adipocytes and stromal-vascular fractions of rat white and brown adipose tissues. FEBS Lett 1999;464: 184-8.
[54] Atzmon G, Yang XM, Muzumdar R, Ma XH, Gabriely I, Barzilai N. Differential gene expression between visceral and subcutaneous fat depots. Horm Metab Res 2002;34:622-8.
[55] Shyu AB, Wilkinson MF, van Hoof A. Messenger RNA regulation: to translate or to degrade. EMBO J 2008;27:471-81.
[56] Zhang C. MicroRNomics: a newly emerging approach for disease biology. Physiol Genomics 2008;33:139-47.
[57] Taleux N, Guigas B, Dubouchaud H, Moreno M, Weitzel JM, Goglia F, et al. High expression of thyroid hormone receptors and mitochondrial glycerol-3-phosphate dehydrogenase in liver is linked to enhanced fatty acid oxidation in Lou/C, a rat strain resistant to obesity. J Biol Chem 2009;284:4308-16.
[58] Wang Y-X, Zhang C-L, Yu RT, Cho HK, Nelson MC, Bayuga-Ocampo CR, et al. Regulation of muscle fiber type and running endurance by PPARδ. PLoS Biology 2004;2:1532-9.
[59] Wang Y-X, Lee C-H, Tiep S, Yu RT, Ham J, Kang H, et al. Peroxisome-proliferator-activated receptor δ activates fat metabolism to prevent obesity. Cell 2003;113:159-70.
[60] Barbera MJ, Schlüter A, Pedraza N, Iglesias R, Villarroya F, Giralt M. Peroxisome proliferator-activated receptor α activates transcription of the brown fat uncoupling protein-1 gene. A link between regulation of the thermogenic and lipid oxidation pathways in the brown fat cell. J Biol Chem 2001;276:1486-93.
[61] Frayn KN, Langin D, Karpe F. Fatty acid-induced mitochondrial uncoupling in adipocytes is not a promising target for treatment of insulin resistance unless adipocyte oxidative capacity is increased. Diabetologia 2008;51:394-7.
[62] Granneman JG, Li P, Zhu Z, Lu Y. Metabolic and cellular plasticity in white adipose tissue I: effects of β3-adrenergic receptor activation. Am J Physiol Endocrinol Metab 2005;289:E608-E616.
[63] Silva JE, Bianco SDC. Thyroid-adrenergic interactions: physiological and clinical implications. Thyroid 2008;18:157-65.
[64] Zubay G. Aerobic production of ATP: electron transport. In: Rogers B, Mirski M, Madru JK, editors. Biochemistry. New York: Addison-Wesley Publishing Company, Inc; 1983. p. 363-407.
[65] Flowers MT, Ntambi JM. Role of stearoyl-coenzyme A desaturase in regulating lipid metabolism. Curr Opin Lipidol 2008;19:248-56.
[66] Flowers MT, Ntambi JM. Stearoyl-CoA desaturase and its relation to high-carbohydrate diets and obesity. Biochim Biophys Acta 2009; 1791:85-91.
[67] Miyazaki M, Flowers MT, Sampath H, Chu K, Otzelberger C, Liu X, et al. Hepatic stearoyl-CoA desaturase-1 deficiency protects mice from carbohydrate-induced adiposity and hepatic steatosis. Cell Metab 2007;6:484-96.
[68] Cao H, Gerhold K, Mayers JR, Wiest MM, Watkins SM, Hotamisligil GS. Identification of a lipokine, a lipid hormone linking adipose tissue to systemic metabolism. Cell 2008;134:933-44.
[69] Solanes G, Pedraza N, Calvo V, Vidal-Puig A, Lowell BB, Villarroya F. Thyroid hormones directly activate the expression of the human and mouse uncoupling protein–3 genes through a thyroid response element in the proximal promoter region. Biochem J 2005;386: 505-13.

[70] Dulloo AG, Samec S. Uncoupling proteins: do they have a role in body weight regulation? News Physiol Sci 2000;15:313-8.
[71] Clapham JC, Arch JR, Chapman H, Haynes A, Lister C, Moore GB, et al. Mice overexpressing human uncoupling protein–3 in skeletal muscle are hyperphagic and lean. Nature 2000;406:415-8.
[72] Seifert EL, Bézaire V, Estey C, Harper M-E. Essential role for uncoupling protein–3 in mitochondrial adaptation to fasting but not in fatty acid oxidation or fatty acid anion export. J Biol Chem 2008;283: 25124-31.
[73] Huffman DM, Barzilai N. Role of visceral adipose tissue in aging. Biochim Biophys Acta 2009;1790:1117-23.
[74] Koh EH, Park JY, Park HS, Jeon MJ, Ryu JW, Kim M, et al. Essential role of mitochondrial function in adiponectin synthesis in adipocytes. Diabetes 2007;56:2973-81.